Womersley Number-Based Estimates of Blood Flow Rate in Doppler Analysis: *In Vivo* Validation by Means of Phase-Contrast MRI

Raffaele Ponzini*, Christian Vergara, Giovanna Rizzo, Alessandro Veneziani, Alberto Roghi, Angelo Vanzulli, Oberdan Parodi, and Alberto Redaelli

Abstract—A common clinical practice during single-point Doppler analysis is to measure the centerline maximum velocity and to recover the time-averaged flow rate by exploiting an assumption on the shape of velocity profile (*a priori* formula), either a parabolic or a flat one. In a previous study, we proposed a new formula valid for the peak instant linking the maximum velocity and the flow rate by including a well-established dimensionless fluid-dynamics parameter (the Womersley number), in order to account for the hemodynamics conditions (*Womersley number-based* formula). Several *in silico* tests confirmed the reliability of the new formula. Nevertheless, an *in vivo* confirmation is missing limiting the clinical applicability of the formula. An experimental *in vivo* protocol using cine phase-contrast MRI (2-D PCMRI) technique has been designed and applied to ten healthy young volunteers in three different arterial districts: the abdominal aorta, the common carotid artery, and the brachial artery. Each PCMRI dataset has been used twice: 1) to compute the value of the blood flow rate used as a gold standard and 2) to estimate the flow rate by measuring directly the maximum velocity and the diameter (i.e., emulating the intravascular Doppler data acquisition) and by applying to these data the *a priori* and the *Womersley number-based* formulae. All the *in vivo* results have confirmed that the *Womersley number-based* formula provides better estimates of the flow rate at the peak instant with respect to the *a priori* formula. More precisely, mean performances of the *Womersley number-based* formula are about three times better than the *a priori* results in the abdominal aorta, five times better in the common carotid artery, and two times better in the brachial artery.

Index Terms—Blood flow, Doppler estimate, doppler ultrasound, phase-contrast MRI (PCMRI), Womersley number.

I. INTRODUCTION

THE DOPPLER-BASED instrumentation measures blood velocity through a section, by acquiring the difference in frequency between a transmitted wave and the reflected signal (Doppler-shift effect). In the *single-point Doppler* method, the reflected signal is retrieved in a single point of the vascular section, so that only the measure of the blood velocity in a selected point of the section is available [55]. The standard practice is to get this measure as the *maximum velocity* V_M over the section. In particular, if the acquisition procedure can be performed in sites sufficiently far from branching, bending, and strongly tapered regions, a symmetry of the velocity profile can be considered (*cylindrical symmetry hypothesis*), so that the measurements of the *centerline velocity* gives a good estimate of the maximum velocity V_M. In these cases, it is usually assumed that the flow rate can be obtained from the maximum velocity, making an *a priori* assumption on the velocity profile (namely, *parabolic* or *flat*). This approach, hereafter referred to as *a priori approach*, has been validated for time-averaged blood flow-rate estimation in the coronaries (see [10]). Successively, it has been applied to a wide range of vascular districts (see, e.g., [21], [36], [45]–[47], and [54]) and under very different blood flow conditions (e.g., baseline and atrial pacing, see, e.g., [19] and [25]). Even if the time-averaged blood flow (estimated from the time-averaged maximum velocity) is commonly used for clinical purposes, sometimes the *peak flow rate* (that is the maximum flow rate over the cardiac cycle) has been considered when changes on blood flow quantities after induced hyperemic stimulus with respect to their basal values are evaluated. The more relevant clinical example is the study of ischemic artery disease, where the ratio of peak velocity during stress-induced maximal coronary vasodilatation to the resting peak velocity [i.e., the coronary flow reserve (CFR)] is considered a well-established indicator of functional effect of coronary stenosis, with direct implications on revascularization interventions (see [18], [19], and [38]). Moreover, the peak flow rate has been

*R. Ponzini is with the High Performance Computing Division, Consorzio Interuniversitario Lombardo per l'Elaborazione Automatica, Segrate (MI) 20090, Italy (e-mail: ponzini@cilea.it).

C. Vergara is with the Department of Information Engineering and Mathematical Methods, Università degli Studi di Bergamo, Bergamo 24129, Italy (e-mail: christian.vergara@unibg.it).

G. Rizzo is with the Institute of Molecular Bioimaging and Physiology, National Research Council, Segrate (MI) 20090, Italy, and also with the Department of Nuclear Medicine, Scientific Institute San Raffaele, Milan 20132, Italy (e-mail: giovanna.rizzo@ibfm.cnr.it).

A. Veneziani is with the Department of Mathematics and Computer Science, and the Wallace H Coulter Department of Biomedical Engineering at Georgia Technical and Emory, Emory University, Atlanta, GA 30322 USA (e-mail: ale@mathcs.emory.edu).

A. Roghi is with the Department of Cardiology and Cardiac Surgery, Niguarda Ca' Granda Hospital, Milan 20162, Italy (e-mail: alberto.roghi@ospedaleniguarda.it).

A. Vanzulli is with the Ca' Granda Niguarda Hospital, Milano 20162, Italy (e-mail: angelo.vanzulli@ospedaleniguarda.it).

O. Parodi is with the Institute of Clinical Physiology, National Research Council, Pisa 56126, Italy, and also with the Ca' Granda Niguarda Hospital, Milano 20162, Italy (e-mail: oberpar@tin.it).

A. Redaelli is with the Department of Bioengineering, Politecnico di Milano, Milano 20133, Italy (e-mail: alberto.redaelli@polimi.it).

Color versions of one or more of the figures in this paper are available online at http://ieeexplore.ieee.org.

Digital Object Identifier 10.1109/TBME.2010.2046484

used also in other clinical applications, see, e.g., [3], where it has been used to evaluate the renal blood flow reserve.

At any instant along the cardiac cycle, the shape of the spatial velocity profile is not known *a priori* (see, e.g., [23] and [24]). Indeed, it is known that, despite the validity of the cylindrical symmetry hypothesis, the shape of the velocity profile is influenced by many factors, including pulsatility, viscosity, and diameter in vascular districts (see [33], [48], and [56]). In general, the velocity profile is not parabolic. For what concerns the time-averaged flow rate, different opinions have been pointed out concerning this assumption. For example, in [11], it has been argued that for a fully developed flow, the time-averaged mean velocity is equal to half the time-averaged maximum velocity, and then, the parabolic assumption seems to be reasonable. In contrast, in [23], [24], and [44], it has been shown that the parabolic assumption could lead to a systematic error also in straight vessels and far from bending or tapered regions. For what concerns the peak flow rate, in [43], it has been shown by means of *in silico* experiments that the parabolic assumption leads to a significant error in the estimation of the flow rate. For this reason, in [43] and here, we have focus on the peak instant, being the flow rate at that instant more critical to be estimated starting from the knowledge of just the maximum velocity.

We have proposed a new formula for the estimation of the flow rate at the peak instant in Doppler analysis starting from the knowledge of V_M in [43]. This formula can be considered as a generalization of the *a priori* method. In particular, it is based on the assumption that the relationship between flow rate and maximum velocity at the peak instant can be better established by taking into account the hemodynamics conditions represented by the *Womersley number*. The latter is a dimensionless parameter depending on the heart pulsatility, the blood viscosity, and the vessel diameter. For this reason, in what follows, this method will be referred as *Womersley number-based* approach (see Appendix for details). This method has been validated *in silico* in both simplified and realistic geometries [carotid bifurcation, Y-shaped bypass grafts, total cavopulmonary connection (TCPC)] studying different flow waveform under a wide range of clinical conditions (baseline and atrial pacing). In all, the *in silico* validations, the advantage of the Womersley number-based formula has been clearly demonstrated suggesting that the new formula performs significantly better at the same cost. Some of these results indicate also that, under certain hemodynamics conditions, the performances of the Womersley number-based formula can be up to five times better with respect to the *a priori* formula, highlighting potentially critical side effects on clinical measurement procedure (see [43]). Nevertheless, even the most sophisticated *in silico* analysis is, however, a simplification of the simulated biological phenomena. Therefore, wondering to propose this formula for clinical usage, first of all, an accurate controlled *in vivo* study was necessary.

To this aim, in this paper, we present an *in vivo* validation of the Womersley number-based formula, by means of 2-D cine phase-contrast MRI (PCMRI). In general, this imaging technique is considered the state-of-the-art to perform local hemodynamics characterization (see [6], [13]–[15], [17], [22], [35], [39], [40], [49], and [53]). Moreover, concerning
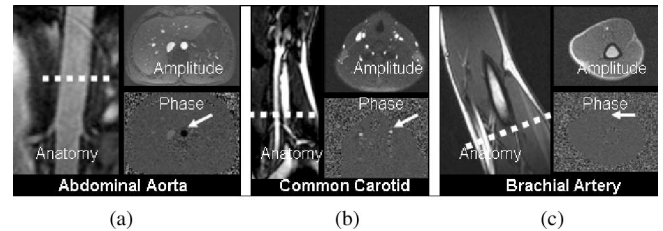

Fig. 1. Anatomical and phase images of the three anatomical district for one volunteer. (a) Abdominal aorta. (b) Common carotid artery. (c) Brachial artery. For each district, the MR anatomical image and the two PC images (amplitude and phase) in the sampled 2-D slice are shown.

the scopes of this study, the choice of PCMRI technique is effective also for three reasons. First, it allows to visually select the sampling plane within the vascular anatomy far from region with branches or bends. Second, it allows to perform simultaneously both geometrical and fluid-dynamics data measurements [2], [7]–[9], [12], [16], [30]–[32], [34], [35], [50], without the usage of any endovascular device or contrast agent that can potentially alter the blood flow. Last, it is widely accepted that under correct sampling condition, the velocity values acquired with this technique are equivalent to those acquired using ultrasound-based techniques [27], [29], [37], [52].

II. MATERIAL AND METHODS

A. PCMRI: Study Design

Ten healthy young volunteers (with age varying between 25–42 years, weight 60–95 kg, all males) have been acquired under baseline conditions using a cine PCMRI protocol for a total scan duration equal to 40 min. All the volunteers signed an informed consent according to the ethic institutional review board of the Niguarda Ca' Granda Hospital (Milan, Italy). Arterial pressure was measured before the acquisition and after the overall protocol to ensure stable hemodynamics conditions and parameters. The baseline measurements have been acquired leaving the subject in resting condition before entering in the MRI chamber for a sufficient amount of time (about 5 min).

We have considered three anatomical sites with different cross-sectional area and located at different levels of the arterial tree, sampling most of the physiological range of the Womersley number in humans. Moreover, we excluded branching or strongly tapered sites, so that assumptions behind the *a priori* approach (i.e., the *cylindrical symmetry hypothesis*) are satisfied. More precisely, the *brachial artery*, the *common carotid artery*, and the *descending aorta* have been chosen to represent small, medium, and large vessels, respectively. Fig. 1 shows samples of the three anatomical sites in one representative volunteer. For each volunteer, we acquired the abdominal aorta and common carotid data under supine position, while the brachial artery data have been acquired under prone position to ensure maximum stability and comfort, and an optimal centering in the main magnetic field accordingly to the MR technician experience. On each arterial district, the scan acquisition took about 10 min.

TABLE I
PCMRI ACQUISITION PROTOCOL

Arterial district	TR [ms]	TE [ms]	Pixel size [mm]	Slice thikness [mm]	Cardiac phases
Abdominal aorta	30.8	4.0	0.8	5.0	30
Common carotid	83.9	4.7	0.7	3.0	20
Brachial	77.0	4.1	0.4	3.0	15

The abdominal aorta, the common carotid artery, and the brachial artery have been acquired using 2-D cine PCMRI technique. For each arterial district the main MRI acquisition parameters are reported.

B. PCMRI: Acquisition Procedure

The region of interest (ROI) was centered as much as possible within the field of view (FOV). 2-D PC data have been acquired using an MR Siemens Magnetom Avanto 1.5T scanner equipped with a 12-channel cardiac phased-array coil and with gradient of maximum intensity equal to 45 mT/m and slew rate equal to 200 T/m/s. The pulse sequence for 2-D cine PCMRI data acquisition was T1-weighted, with flip angle set to 30°. The other sequence parameters such as the repetition time (TR) and echo time (TE), as well as image spatial and temporal resolution have been adapted for the different vessels in order to preserve a detailed in-plane spatial accuracy and assuming the total scan time to be constant. In particular, the in-plane pixel values ranges from 0.4 to 1 mm according to the different size of the vascular districts. A single velocity component aligned to the vessel axis was acquired, with velocity encoding along the direction orthogonal to the slice orientation ("through-plane" encoding). The acquisition was synchronized to the cardiac cycle, using the ECG signal as trigger and a beat rejection of $\pm 10\%$; a retrospective gating algorithm, as implemented in the scanner acquisition protocols, was used to generate images corresponding to the selected number of cardiac phases. Due to retrospective gating, heart rate variations occurred during acquisition are identified and used to remap the single R–R period to a mean R–R duration [20]. In Table I, the specific acquisition parameters set for each arterial districts are shown. For each subject and in each district, a preliminary encoding velocity scout sequence has been performed for optimizing the value of such velocity, namely the V_{enc}, out of three possible values. This preliminary sequence allowed us to avoid any aliasing artefacts in the final phase image.

C. Data Processing

The phase images were segmented in order to extract wall vessels location, using a semiautomatic method previously proposed and validated in [1].

After the segmentation process, as suggested in [41], we performed a further processing of the images as shown in Fig. 2, where the overall flowchart of the validation protocol is presented. At the peak velocity time frame, the segmented PCMRI images have been used in two ways.

1) The entire spatial velocity profile has been used for retrieving an accurate flow-rate measure. This has been used as gold standard value (Q_{GS}), denoted as *computed flow rate*.
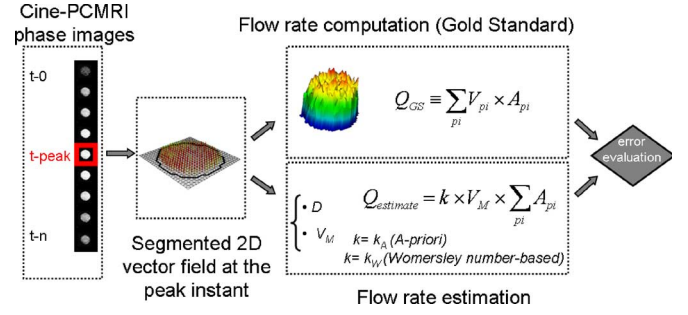

Fig. 2. *In vivo* protocol scheme. At the peak velocity instant the PCMRI dataset has been used in two ways. (Top) PCMRI blood flow-rate computation (Q_{GS} gold standard). (Bottom) Flow-rate estimates using the *a priori* (Q_A) and the *Womersley number-based* (Q_W) approaches.

The gold standard value Q_{GS} of the blood flow rate has been computed by numerical integration over the artery cross-sectional area of the local velocity field V_{pi} taken on each pixel (pi) of the lumen. More precisely, we set

$$Q_{\mathrm{GS}} = \sum_{\mathrm{pi}} V_{\mathrm{pi}} A_{\mathrm{pi}} \qquad (1)$$

where A_{pi} is the area of the single intravessel pixel (pi).

2) The maximum velocity V_M and the diameter D of the section at hand have been used for estimating the flow rate Q through this section, mimicking the intravascular Doppler analysis. In particular, we compute both the *a priori* estimate (Q_A) and the Womersley number-based one (Q_W). We will call these values *estimated flow rates*.

In particular, the *a priori* formula consists in the following equation:

$$Q_A = k_A V_M \sum_{\mathrm{pi}} A_{\mathrm{pi}} \qquad (2)$$

where

$$k_A = 0.5, \ \text{for parabolic profile}$$

$$k_A = 1, \ \text{for parabolic profile}$$

while the Womersley number-based formula, read as follows:

$$Q_W = k_W V_M \sum_{\mathrm{pi}} A_{\mathrm{pi}} \qquad (3)$$

where k_W depends on the Womersley number W and is defined in the Appendix.

For all the estimations in the subjects, a constant values of blood viscosity (3.5 mPa·s) and density (1060 kg/m^3) have been assumed, according to the fact that all the volunteers, where healthy subjects. In Table IV in the Appendix of the paper, the values (mean $\pm$ std) of k_w found in the three districts for the ten volunteers are summarized.

D. Statistical Analysis

The Bland–Altman test is a clinical indicator of the equivalence of two different measure procedures for the same quantity and it has been proved to able to quantify their correlations [5]. Here, the Bland–Altman test has been performed in order to

TABLE II
In Vivo MEASUREMENTS

Arterial district	Vessel diameter D [cm]	Maximum velocity V_{GS} [cm/s]	Womersley number W	Gold standard flow rate Q_{GS} [cm³/s]
Abdominal aorta	1.90 +/- 0.15	104.76 +/-14.65	13.0 +/- 1.0	236.21+/- 40.02
Common carotid	0.69 +/- 0.04	80.06 +/-13.10	4.7 +/- 0.3	19.17 +/- 3.41
Brachial	0.43 +/- 0.05	57.26 +/- 11.9	3.0 +/- 0.3	4.89 +/- 1.24

In vivo measures of interest at the peak velocity instant for the three districts (mean ± std).

establish the reliability of the two estimates formulae (namely, the *a priori* and the Womersley number-based). In particular, the two estimates (Q_A and Q_W) have been compared to the reference value Q_{GS}.

III. RESULTS

With reference to Fig. 2, the values of the estimated flow rates at the peak instant [Q_A and Q_W, (2) and (3)] have been computed, and then, compared to their associated gold standard values Q_{GS} [see (1)] for a total of 30 observations (three district for ten volunteers), covering a range of the Womersley number between 2.5 and 14.7. We point out that we use the flat assumption in the *a priori* formula only for the dataset collected in the abdominal aorta, where a parabolic hypothesis is known to be unreliable and a flat profile is commonly hypothesized.

A. Blood Flow Velocity Measurements and Flow-Rate Estimates

In Table II, we summarize the measures of interest for the purposes of this analysis obtained from the *in vivo* data after the segmentation process. Namely, the maximum velocity [V_M in centimeter per second], the vessel diameter (D in centimeter), the Womersley number W, and the gold standard flow rate (Q_{GS} in cubic centimeter per second) have been sampled at the peak instant. The three districts clearly feature separated values of V_M, D, W, and Q_{GS}, as highlighted by their mean values.

In Fig. 3, the estimated flow rates Q_A and Q_W [see (2) and (3)] together with the gold standard Q_{GS} [see (1)] for all the 30 cases are shown.

B. Statistical Analysis

In Table III, we report for the two formulae a synthesis of the percentage differences, in terms of mean value and variance, in the three arterial districts.

In Fig. 4, we report the result of the Bland–Altman test [5]. On the horizontal-axis, we report the average between the gold standard and the estimated flow rates, on the vertical-axis, we report their differences. The solid line indicates the mean values of the differences, the dashed one indicates the variance. The results obtained with the *a priori* and with the Womersley number-based formulae are shown in the left and right column, respectively. Considering the very different behavior of the three vascular districts, from the top of the figure to the bottom, we report the results of the test performed on the overall dataset
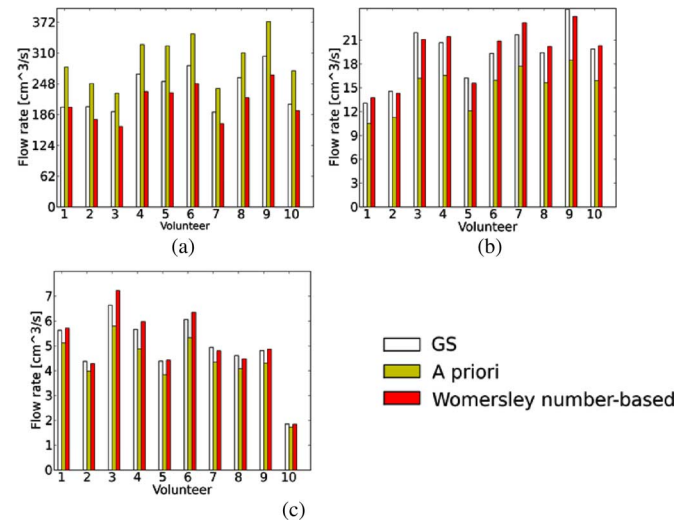

Fig. 3.　Estimated and computed flow rates. For all the 30 volunteers, the result of the *in vivo* data processing is shown. The estimated flow rates Q_A and Q_W [see (2) and (3)] in cubic centimeter per second are plotted together with the computed gold standard Q_{GS} [see (1)]. All the data are in cubic centimeter per second. (a) Abdominal aorta. (b) Common carotid artery. (c) Brachial artery.

TABLE III
OVERALL STATISTICAL ANALYSIS OF THE TWO ESTIMATE'S APPROACHES

Arterial district	A-priori	Womersley number-based
Abdominal aorta	25.4 +/- 6.2	10.9 +/- 4.5
Common carotid	21.5 +/- 3.0	4.2 +/- 1.8
Brachial	11.1 +/- 2.0	3.1 +/- 2.5

Mean ± std of the percentage errors (in percent) between the estimates and the gold standard value using the *a priori* and the Womersley number-based formula in the three arterial districts.

(panel a) and on each single dataset (abdominal aorta, carotid artery, and brachial artery on panels *b, c,* and *d*, respectively).

C. Visualization of Spatial Velocity Profiles

To get a visualization of the velocity data acquired with PCMRI in the three districts at the peak velocity instant, in Fig. 5, we report the 3-D spatial velocity profiles for three subjects. From these images, we observe that the profiles are fairly cylindrically symmetric. However, they are only roughly parabolic or flat. This is highlighted in the right panel of Fig. 5, where for one representative subject, we have compared the acquired velocity profile across a single diameter (2-D) with the corresponding parabolic (flat for the abdominal aorta) profile, featuring the same value of the centerline velocity.

IV. DISCUSSION

A. Doppler-Like Analysis: Blood Flow-Rate Estimates and Spatial Velocity Profiles

The main finding of this paper, as shown by the results in Fig. 3 and Table III, is that the Womersley number-based formula better estimates the flow rate with the respect to the *a priori* formula in all the 30 evaluation. This confirms previous observations found in [43]. In particular, the *a priori* approach leads to a systematic underestimation or overestimation of the
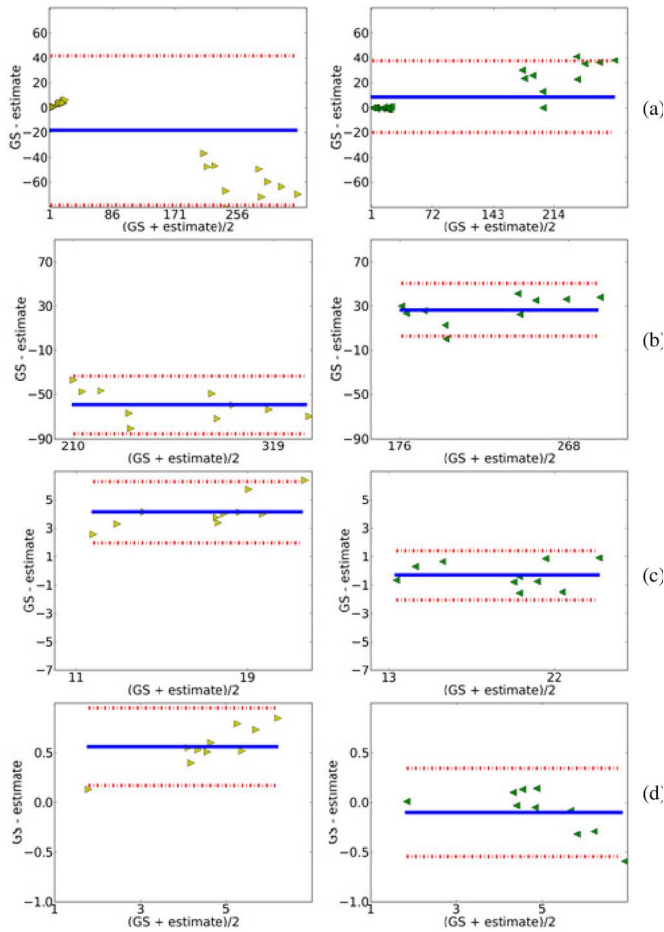
Fig. 4. Bland–Altman test. The results obtained with the *a priori* approach are reported on the left (the flat hypothesis has been used only for the abdominal aorta data), the results of the *Womersley number-based* approach on the right. The statistical analysis has been performed considering all the three districts together and for each single vascular district. (a) Complete dataset. (b) Abdominal aorta. (c) Carotid artery. (d) Brachial artery. All the data are in cubic centimeter per second.
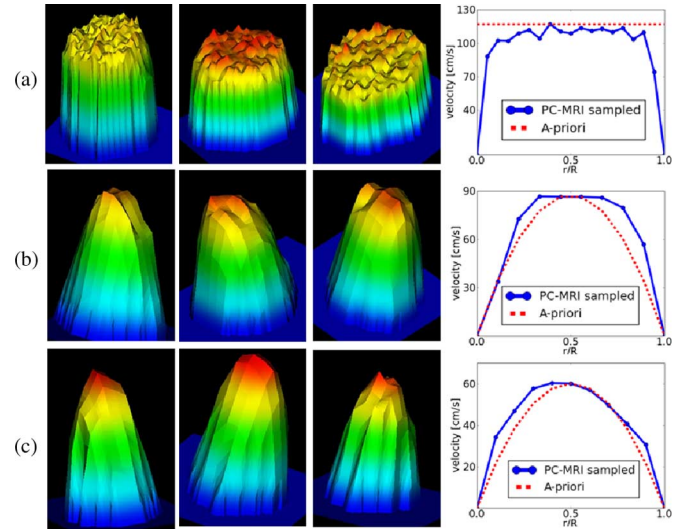

Fig. 5. 3-D/2-D spatial velocity profiles. (a) Abdominal aorta. (b) Common carotid artery. (c) Brachial artery. To get a simpler visualization of the changes of the spatial velocity profiles (in centimeter per second) at different Womersley number values, the sampled 2-D velocity profiles across a single (normalized) diameter in each district are shown for a single representative subject, and compared with a parabola (flat profile for the aorta) sharing the same value of maximum velocity V_M (vertex of the parabola, in centimeter per second).

flow rate for the parabolic and flat assumptions, respectively. For example, the *a priori* formula in small-sized vessels (mean diameter equal to 0.43 cm in our dataset–parabolic approximation) is affected by a mean relative error of 11.1%, while the Womersley number-based one features 3.1%. For the medium- and large-sized vessels (mean diameter equal to 0.69 and 1.90 cm, respectively), the mean relative errors are 21.5% and 25.4% for the *a priori* formula and 4.2% and 10.9% for the Womersley number-based one. Therefore, in the three typologies of districts, the mean performances of the Womersley number-based formula are about 3, 5, and 2 times better than the ones obtained by the *a priori* formula, respectively. In synthesis, the performances of the two formulae (see Table III) confirm that the Womersley number-based one is able to provide remarkably better performances also *in vivo*.

The statistical analysis provided by the Bland–Altman method (see Fig. 4) also confirms that the Womersley number-based formula is more reliable than the *a priori* one. Indeed, considering the results on the overall dataset [see Fig. 4(a)], the

absolute value of the mean error is clearly lower with a smaller variance (8.2 ± 28.3 cm^3/s for the Womersley number-based versus -19.1 ± 61.4 cm^3/s for the *a priori* one). The results of each vascular districts show that in the brachial and the carotid artery, the Womersley number-based formula has a full level of equivalence with the gold standard (being the absolute value of the mean difference in the two districts equal to 1.44 and 0.34 cm^3/s respectively), while the *a priori* formula features a sensible underestimation bias in both the arterial districts (being the absolute value of the mean difference equal to 6.29 and 0.95 cm^3/s) [see Fig. 4(c) and (d)].

As a matter of fact, the assumptions behind the *a priori* approach are unreliable, as shown by the visualization of the 3-D spatial velocity profiles at the peak velocity instant (see Fig. 5). In Fig. 5, we compare also the acquired velocity profile across a single diameter with the corresponding parabolic (or flat for the abdominal aorta) profile, featuring the same value of the centerline velocity. It is evident that despite the reliability of the *cylindrical symmetry hypothesis,* the velocity profiles assumed in the *a priori* approach are not accurate.

B. Dependence of the Error on W

In Fig. 6, the relative error, with respect to the gold standard value, is reported as function of the Womersley number for the *a priori* estimates. Considering the overall trend of the *a priori* approach, we observe that the absolute value of the error increases as the values of W get larger. This explains why the introduction of the Womersley number in the formula improves the estimates.
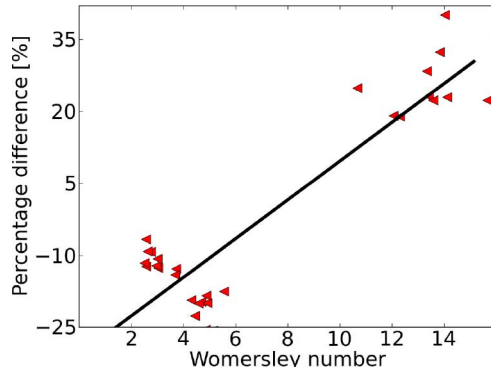
Fig. 6. Percentage errors of the *a priori* formula is shown as function of the Womersley number values together with the linear regression line.

TABLE IV
k_w VALUES

Arterial district	k_w
Abdominal aorta	0.7 +/- 0.01
Common carotid	0.65 +/- 0.01
Brachial	0.58 +/- 0.03

The mean value and the standard deviation of the k_w values used for the computation in (3) is shown for the three arterial districts studied.

C. Possible Clinical Applications

The Womersley number depends on the diameter, heart rate, and viscosity. In this study, the viscosity has been assumed to be constant among all the subjects, while the diameter varies in the range 0.38–2.14 cm, and the heart rate in 56.8 ± 6.2 beats per minute (bpm). Therefore, in the results presented in the previous section, the variation on the shape of the spatial velocity profile is mainly due to the variability of the diameter. In particular, the results reported in Figs. 3 and 6 show that the error of the *a priori* approach becomes higher (as absolute value) when D (and then W) increases, whilst with the Womersley number-based approach, they are confined below 15.75%. Therefore, we can state that the *a priori* approach is, in particular, not recommended in medium and large vessels.

It is well known that the velocity profile depends on the Womersley number (see [56] for a theoretical discussion), which increases when the heart rate increases. Therefore, we expect that the performances of the *a priori* formula deteriorate when the heart rate increases, in analogy with the case of increasing diameter, since in both cases, the Womersley number increases (see Fig. 6). On the contrary, (3), which depends on the Womersley number (and consequently on the heart rate), should provide significant better estimates of the flow rate, also for higher heart rates. This could have relevant clinical implications. For example, it could lead to better estimates of the CFR, being this quantity crucial in interventional clinics, since it has been extensively used to assess coronary vasodilating capability in patients with suspected or known coronary artery disease (CAD) (see [18], [19], [28], and [38]). Of course, a validation of the performances of the Womersley-number based formula for high heart rate should be directly performed. This will be the object of a future study.

Finally, we can state that this formula will be able to help also other new future applications, where the peak flow rate is of some clinical interest.

D. Data Requirements

For the application of the Womersley number-based formula, only the measurement of the vessel diameter, viscosity, and the maximum velocity are needed (see Appendix for further details

on the Womersley number calculation *in vivo*). Therefore, this strategy does not require any new data with respect to those already acquired during a typical Doppler analysis (see [41]–[43], and [51]). The application of (3) is therefore immediate in practice. Indeed, in [51], this formula has been applied, without any new acquisition, to a velocimetry Doppler dataset to provide a CFR evaluation. From this point of view, our formula provides an algebraic expression that is comparable to the complexity of the *a priori* formula. Other approaches are based on the application of the Womersley theory (that is on the analytical expression of the flow rate in terms of velocity, see [4], [26], and [56]). These methods are certainly elegant and sophisticated, however, they feature a higher mathematical complexity (in performing fast Fourier transform (FFT) and managing Bessel functions) in comparison with the *a priori* formula that involve just a multiplication of V_M by a constant factor (0.5 or 1.0). In our formula, the value of V_M is multiplied by a parametric factor that depends on the Womersley number (see Table IV in the Appendix for the k_W values (mean $\pm$ std) found for the ten volunteers in the three districts). Even more important, the Womersley theory is exact only in cylindrical domains, whilst a Womersley-number formula could be, in principle, obtained for any district, provided that suitable numerical simulations in those districts are performed (see [43]). Indeed, due to the modern geometry reconstruction techniques, it is nowadays possible to perform numerical simulations in any vascular domain. However, a more detailed comparison between the approach based on the Womersley theory, and the one presented and validated, in this paper, will be carried out extensively as a future development of this study.

E. Blood Rheology

The viscosity of blood has been considered to be constant for all subjects. This hypothesis is justified by theoretical and clinical observations, as discussed in [51], where it has been shown the negligible dependence of the flow-rate estimate on the rheology model.

V. LIMITATIONS AND CONCLUSION

There are several limitations and possible extensions to this study.

1) The value of V_M has been obtained still using PCMRI. Obviously, a more effective comparison between the different estimated flow rates could be performed by acquiring the

value of V_M with a Doppler technique. However, this would introduce a bias in the two measurements due to possible different physiological conditions of the subject during the two acquisitions that could not be acquired at the same instant. For this reason, we decided to process the value of V_M acquired with the PCMRI, yielding the gold standard computations and the estimates from measures acquired at the same time. Moreover, it is worth to underline that, under correct sampling condition, the velocity values acquired with ultrasound-based techniques and using cine PCMRI are equivalent as stated in [27], [29], [37], and [52]. Being our *in vivo* analysis oriented on the study of arterial sites far from bends and or branching, where the velocity patterns are highly axial and undisturbed, we can state that the acquisition of the maximum velocity with the PCMRI did not alter the results one would obtain by using directly the ultrasound procedure.

2) As pointed out in Section II, we resorted to a robust segmentation method, guaranteeing a good level of operator independence. A possible further step for reducing uncertainty from gold standard values is to resort to an *in vitro* validation using MRI pulsatile flow phantoms.

3) Our investigation does not sample values in the interval of the Womersley number between 5.9 and 11.8. Unfortunately, this was not under the control of the authors, since all the acquisition have been done under baseline conditions, and then, without the possibility to modify the heart rate over the physiological intersubject variability to fill out all the range of W.

Despite of these limitations and possible improvements, this study confirms with the proposed *in vivo* validation that the new Womersley number-based formula for estimating blood flow from the measurement of V_M is by far better than the traditional ones at the same cost, i.e., without requiring any different or new acquisition procedures.

It is finally worth to mention that Womersley number-based formula is the result of a statistical analysis conducted over hundreds of numerical simulations performed in [43] (see Appendix). The reliability of this analysis can be, therefore, further improved in two ways.

1) Equation (3) has been devised with a "general purpose" perspective, i.e., covering a wide (physiological) range of Womersley number. If the Womersley numbers of interest refer to a limited interval, an *ad hoc* formula can be devised with the same procedure, so that in the range of interest flow-rate estimations can be further enhanced (see [43]).

2) The approach could be extended to the whole cardiac cycle. This would require to include the sampling of the maximum velocity over the cardiac cycle, thus allowing an estimate of the time-averaged flow rate.

APPENDIX

The flow rate through a section Γ is defined as follows:

$$Q = \int_{\Gamma} u n \, d\gamma \tag{A1}$$

where u is the blood velocity and n is the normal unit vector. In order to obtain Q, the whole spatial velocity profile is needed. However, the flow rate can be approximated by the formula as follows:

$$Q = k V_M A \tag{A2}$$

for a suitable value of k. For example, in a cylinder in steady conditions, we have $k = 0.5$ (parabolic profile). However, this value is not correct for not cylindrical domains (even if the *cylindrical symmetry hypothesis* is satisfied) and/or in pulsatile conditions. For this reason, other values of k need to be found in order to get a better estimate of the flow rate. However, this *a priori* choice of k is not satisfactory in the general case.

A possible keypoint to generalize the *a priori* approach is to consider the hemodynamics conditions by including the Womersley number in the flow-rate estimation. The Womersley theory has been developed by Womersley [56] for a single-sinusoidal pressure drop applied over a cylindrical rigid-wall geometry for the calculation of velocity, rate of flow, and viscous drag in arteries when the pressure gradient is known. In this paper, the expression of a dimensionless fluid dynamics quantity (Womersley number W) is given

$$W = D \sqrt{\frac{f \pi}{2 \nu}} \tag{A3}$$

where f is the frequency and ν is the blood viscosity.

In this paper, the application of the Womersley theory to the case of measured pressure curves (femoral dog) is discussed. In this case, the author explains how to decompose a complex measured signal into the summation of sinusoidal contribution due to the Fourier theory (harmonics decomposition). For each harmonic contribution, a specific value of W can be computed, and used separately and independently from the contribution of the other harmonics (principle of superimposing effect). Nevertheless, in the work of Womersley [56], it is also clearly mentioned that a unique and representative value of W can be calculated for a specific arterial district (in the paper, where the case of the human femoral artery is discussed), using the heart rate as reference frequency. Therefore, in this paper, we have computed the Womersley number by referring to this definition, so that the frequency f in (A3) is given by the heart rate.

We have shown that by means of wide computational-based campaign, a new expression for the value of k as a function of the Womersley number can be found in [43]. This strategy stems from the application of a computational fluid dynamics (CFD) technique, where the flow rate is prescribed through the introduction of a Lagrange multiplier (see [43]). Starting from the data arising from a large set of simulations performed with this technique, by means of a Levenberg–Marquand nonlinear least-mean-squares algorithm, a new formula linking the maximum velocity and the flow rate at the peak instant has been proposed. This approach automatically improves the reliability of the estimate procedure. In particular, the following expression has been proposed in [43]:

$$k = k_w = \begin{cases} g_1, & W \leq 2.7 \\ p g_1 + (1-p) g_2, & 2.7 < W \leq 3.1 \\ g_2, & 3.1 < W \leq 15. \end{cases} \tag{A4}$$

where

$$g_1(W) = 0.5(1 + a_1 W^{b_1});$$

$$g_2(W) = 0.5 b_2 \arctan(a_2 W);$$

$$\begin{cases} a_1 = 0.00417 & b_1 = 2.95272 \\ a_2 = 1.00241 & b_2 = 0.94973 \end{cases};$$

and

$$p = e^{(W-2.7)^2/(w-2.7)^2 - (3.1-2.7)^2}.$$

ACKNOWLEDGMENT

REFERENCES

[1] N. Alperin and S. H. Lee, "PUBS: Pulsatility-based segmentation of lumens conducting non-steady flow," *Magn. Res. Med.*, vol. 49, no. 5, pp. 934–944, 2003.

[2] L. Axel, "Blood flow effects in magnetic resonance imaging," *AJR Amer. J. Roentgenol.*, vol. 143, pp. 1157–1166, 1984.

[3] J. P. Beregi, C. Mounier-Vehier, P. Devos, C. Gautier, C. Libersa, E. P. McFadden, and A. Carré, "Doppler flow wire evaluation of renal blood flow reserve in hypertensive patients with normal renal arteries," *Cardiovasc. Int. Radiol.*, vol. 23, no. 5, pp. 340–346, 2000.

[4] J. R. Blake, S. Meagher, K. H. Fraser, W. J. Easson, and P. R. Hoskins, "A method to estimate wall shear rate with a clinical ultrasound scanner," *Ultrasound Med. Biol.*, vol. 34, no. 5, pp. 760–774, 2008.

[5] J. M. Bland and D. G. Altman, "Statistical methods for assessing agreement between two methods of clinical measurement," *Lancet*, no. 8476, pp. 307–310, 1986.

[6] H. G. Bogren, S. R. Underwood, D. N. Firmin, R. H. Mohiaddin, R. H. Klipstein, R. S. Rees, and D. B. Longmore, "Magnetic resonance velocity mapping in aortic dissection," *Br. J. Radiol.*, vol. 61, pp. 456–462, 1988.

[7] D. J. Bryant, J. A. Payne, D. N. Firmin, and D. B. Longmore, "Measurement of flow with NMR imaging using a gradient pulse and phase difference technique," *J. Comput. Assist. Tomogr.*, vol. 8, pp. 588–593, 1984.

[8] C. T. Burt, "NMR measurements and flow," *J. Nucl. Med.*, vol. 23, pp. 1044–1045, 1982.

[9] A. Constantinesco, J. J. Mallet, A. Bonmartin, C. Lallot, and A. Briguet, "Spatial or flow velocity phase encoding gradients in NMR imaging," *Magn. Reson. Imag.*, vol. 2, pp. 335–340, 1984.

[10] J. W. Doucette, P. D. Corl, H. M. Payne, A. E. Flynn, M. Goto, M. Nassi, and J. Segal, "Validation of a Doppler guide wire for intravascular measurement of coronary artery flow velocity," *Circulation*, vol. 85, pp. 1899–1911, 1992.

[11] O. H. Evans, "On the measurement of the mean velocity of blood flow over the cardiac cycle using Doppler ultrasound," *Ultrasound Med. Biol.*, vol. 11, pp. 735–741, 1985.

[12] D. A. Feinberg, L. E. Crooks, P. Sheldon, J. Hoenninger, 3rd, J. Watts, and M. Arakawa, "Magnetic resonance imaging the velocity vector components of fluid flow," *Magn. Reson. Med.*, vol. 2, pp. 555–566, 1985.

[13] D. N. Firmin, G. L. Nayler, P. J. Kilner, and D. B. Longmore, "The application of phase shifts in NMR for flow measurement," *Magn. Reson. Med.*, vol. 14, pp. 230–241, 1990.

[14] D. N. Firmin, G. L. Nayler, R. H. Klipstein, S. R. Underwood, R. S. Rees, and D. B. Longmore, "*In vivo* validation of MR velocity imaging," *J. Comput. Assist. Tomogr.*, vol. 11, pp. 751–756, 1987.

[15] R. Frayne, D. A. Steinman, C. R. Ethier, and B. K. Rutt, "Accuracy of MR phase contrast velocity measurements for unsteady flow," *J. Magn. Reson. Imag.*, vol. 5, pp. 428–431, 1995.

[16] E. L. Hahn, "Detection of sea water motion by nuclear precession," *J. Geophys. Res.*, vol. 65, no. 2, pp. 776–777, 1960.

[17] N. J. Hangiandreou, P. J. Rossman, and S. J. Riederer, "Analysis of MR phase-contrast measurements of pulsatile velocity waveforms," *J. Magn. Reson. Imag.*, vol. 3, pp. 387–394, 1993.

[18] T. Hozumi, K. Yoshida, Y. Ogata, T. Akasaka, Y. Asami, T. Takagi, and S. Morioka, "Noninvasive assessment of significant left anterior descending coronary artery stenosis by coronary flow velocity reserve with transthoracic color Doppler echocardiography," *Circulation*, vol. 97, no. 16, pp. 1557–1562, 1998.

[19] S. Iliceto, V. Marangelli, C. Memmola, and P. Rizzon, "Transesophageal Doppler echocardiography evaluation of coronary blood flow velocity in baseline conditions and during dipyridamole-induced coronary vasodilation," *Circulation*, vol. 83, no. 1, pp. 61–69, 1991.

[20] S. Ley, J. Ley-Zaporozhan, K. F. Kreitner, S. Iliyushenko, M. Puderbach, W. Hosch, H. Wenz, J. P. Schenk, and H. U. Kauczor, "MR flow measurements for assessment of the pulmonary, systemic and bronchosystemic circulation: impact of different ECG gating methods and breathing schema," *Eur. J. Radiol.*, vol. 61, pp. 124–129, 2007.

[21] T. Kamata, M. Moriuchi, S. Saito, Y. Takaiwa, K. Horiuchi, T. Takayama, J. Yajima, T. Shimizu, J. Honye, N. Tanigawa, Y. Ozawa, and K. Kanmatsuse, "Measurement of pulmonary artery flow velocity using a Doppler guidewire," *Jpn. J. Intervent. Cardiol.*, vol. 11, no. 2, pp. 31–37, 1996.

[22] K. A. Kraft, D. Y. Fei, and P. P. Fatouros, "Quantitative phase-velocity MR imaging of in-plane laminar flow: Effect of fluid velocity, vessel diameter, and slice thickness," *Med. Phys.*, vol. 19, pp. 79–85, 1992.

[23] R. Jenni, P. A. Kaufmann, Z. Jiang, C. Attenhofer, A. Linka, and L. Mandinov, "*In vitro* validation of volumetric blood flow measurement using doppler flow wire," *Ultrasound Med. Biol.*, vol. 26, no. 8, pp. 1301–1310, 2000.

[24] R. Jenni, F. Matthews, S. V. Aschkenasy, M. Lachat, B. van Der-Loo, E. Oechslin, M. Namdar, Z. Jiang, and P. A. Kaufmann, "A novel *in vivo* procedure for volumetric flow measurements," *Ultrasound Med. Biol.*, vol. 30, no. 5, pp. 633–637, 2004.

[25] E. L. Johnson, P. G. Yock, V. K. Hargrave, J. P. Srebro, S. M. Manubens, W. Seitz, and T. A. Ports, "Assessment of severity of coronary stenoses using a doppler catheter validation of a method based on the continuity equation," *Circulation*, vol. 80, no. 3, pp. 625–635, 1989.

[26] C. A. D. Leguy, E. M. H. Bosboom, A. P. G. Hoeks, and F. N. van de Vosse, "Model-based assessment of dynamic arterial blood volume flow from ultrasound measurements," *Med. Biol. Eng. Comp.*, vol. 47, no. 6, pp. 641–648, 2009.

[27] S. E. Maier, D. Meier, P. Boesiger, U. T. Moser, and A. Vieli, "Human abdominal aorta: Comparative measurements of blood flow with MR imaging and multigated Doppler U.S," *Radiology*, vol. 171, no. 2, pp. 487–492, 1989.

[28] A. L. McGinn, C. W. White, and R. F. Wilson, "Interstudy variability of coronary flow reserve. Influence of heart rate, arterial pressure, and ventricular preload," *Circulation*, vol. 81, pp. 1319–1330, 1990.

[29] D. Meier, S. Maier, and P. Boesiger, "Quantitative flow measurements on phantoms and on blood vessels with MR," *Magn. Reson. Med.*, vol. 8, no. 1, pp. 25–34, 1988.

[30] P. R. Moran, "A flow velocity zeugmatographic interlace for NMR imaging in humans," *Magn. Reson. Imag.*, vol. 1, pp. 197–203, 1982.

[31] O. C. Morse and J. R. Singer, "Blood velocity measurements in intact subjects," *Science*, vol. 170, pp. 440–441, 1970.

[32] G. L. Nayler, D. N. Firmin, and D. B. Longmore, "Blood flow imaging by cine magnetic resonance," *J. Comput. Assist. Tomogr.*, vol. 10, pp. 715–722, 1986.

[33] W. W. Nichols and M. F. O'Rourke, *McDonald's Blood Flow in Arteries*, 5th ed. London, U.K.: Hodder Arnold., 1990.

[34] M. O'Donnell, "NMR blood flow imaging using multiecho, phase contrast sequences," *Med. Phys.*, vol. 12, pp. 59–64, 1985.

[35] M. Oelhafen, J. Schwitter, S. Kozerke, R. Luechinger, and P. Boesiger, "Assessing arterial blood flow and vessel area variations using real-time zonal phase-contrast MRI," *J. Magn. Reson. Imag.*, vol. 23, pp. 422–429, 2006.

[36] Y. Okada, S. Ono, T. Takizawa, Y. Ishihara, Y. Sugiyama, M. Watanabe, and N. Saegusa, "Assessment of pulmonary artery flow velocity using a Doppler guidewire after the Fontan operation," *Respir. Cir.*, vol. 46, no. 12, pp. 1223–1229, 1998.

[37] S. O. Oktar, C. Yucel, D. Karaosmanoglu, K. Akkan, H. Ozdemir, N. Tokgoz, and T. Tali, "Blood-flow volume quantification in internal carotid and vertebral arteries: Comparison of 3 different ultrasound techniques with phase-contrast MR imaging," *AJNR Amer. J. Neuroradiol.*, vol. 27, no. 2, pp. 363–369, 2006.

[38] I. A. Paraskevaidis, D. P. Tsiapras, Z. S. Kyriakides, and D. Th. Kremastinos, "Transesophageal Doppler evaluation of left anterior descending coronary artery angioplasty," *Amer. J. Cardiol.*, vol. 80, no. 7, pp. 947–951, 1997.

[39] N. J. Pelc, R. J. Herfkens, A. Shimakawa, and D. R. Enzmann, "Phase contrast cine magnetic resonance imaging," *Magn. Reson. Q.*, vol. 7, pp. 229–254, 1984.

[40] N. J. Pelc, F. G. Sommer, K. C. Li, T. J. Brosnan, R. J. Herfkens, and D. R. Enzmann, "Quantitative magnetic resonance flow imaging," *Magn. Reson. Q.*, vol. 10, pp. 125–147, 1994.

[41] R. Ponzini, "Computational modelling of local haemodynamics phenomena: Methods, tools and clinical applications," Ph.D. thesis, Dept. of Bioeng., Politecnico di Milano, Milan, Italy. 2007.

[42] R. Ponzini, M. Lemma, U. Morbiducci, C. Antona, F. M. Montevecchi, and A. Redaelli, "Doppler derived quantitative flow estimate in coronary artery bypass graft: A computational multiscale model for the evaluation of the current clinical procedure," *Med. Eng. Phys.*, vol. 30, no. 7, pp. 809–816, 2008.

[43] R. Ponzini, C. Vergara, A. Redaelli, and A. Veneziani, "Reliable CFD-based estimation of flow rate in haemodynamics measures," *Ultrasound Med. Biol.*, vol. 32, no. 10, pp. 1545–1555, 2006.

[44] G. Porenta, H. Schima, A. Pentaris, S. Tsangaris, D. Moertl, P. Probst, G. Maurer, and H. Baumgartner, "Assessment of coronary stenoses by Doppler wires: A validation study using *in vitro* modeling and computer simulations," *Ultrasound Med. Biol.*, vol. 25, no. 5, pp. 793–801, 1999.

[45] C. Privat, A. Ravel, P. Chirossel, O. Borson, N. Perez, P. Bourlet, L. Walker, J. F. Viallet, and L. Boyer, "Endovascular Doppler guide wire in renal arteries: Correlation with angiography in 20 patients," *Invest. Radiol.*, vol. 34, no. 8, pp. 530–535, 1999.

[46] Rigatelli Gia, M. Barbiero, G. Docali, M. Zanchetta, L. Pedon, A. Baratto, P. Maiolino, Rigatelli Gio, Carraro U, and Dalla Volta S, "Validation of Doppler flow guidewire for peak aortic flow measurement in order to establish its sensitivity for recognition of cardiac assistance in demand dynamic cardiomyoplasty," *Basic Appl. Myol.*, vol. 10, no. 3, pp. 127–130, 2000.

[47] S. J. Savader, G. B. Lund, and F. A. Osterman, "Volumetric evaluation of blood flow in normal renal arteries with a Doppler flow wire: A feasibility study," *J. Vas. Int. Radiol.*, vol. 8, no. 2, pp. 209–214, 1997.

[48] S. Tsangaris and N. Stergiopulos, "The inverse Womersley problem for pulsatile flow in straight rigid tubes," *J. Biomech.*, vol. 21, no. 3, pp. 263–266, 1998.

[49] S. R. Underwood, D. N. Firmin, R. H. Klipstein, R. S. Rees, and D. B. Longmore, "Magnetic resonance velocity mapping: Clinical application of a new technique," *Br. Heart J.*, vol. 57, pp. 404–412, 1987.

[50] P. Van Dijk, "Direct cardiac NMR imaging of heart wall and blood flow velocity," *J. Comput. Assist. Tomogr.*, vol. 171, pp. 429–436, 1984.

[51] C. Vergara, R. Ponzini, A. Veneziani, A. Redaelli, D. Neglia, and O. Parodi, "Womersley number-based estimation of flow rate with Doppler ultrasound: Sensitivity analysis and first clinical application," *Comput. Methods Programs Biomed.*, Oct. 28, 2009. [Epub ahead of print].

[52] A. Vieli, U. Moser, S. Maier, D. Meier, and P. Boesiger, "Velocity profiles in the normal human abdominal aorta: A comparison between ultrasound and magnetic resonance data," *Ultrasound Med. Biol.*, vol. 15, no. 2, pp. 113–119, 1989.

[53] M. F. Walker, S. P. Souza, and C. L. Dumoulin, "Quantitative flow measurement in phase contrast MR angiography," *J. Comput. Assist. Tomogr.*, vol. 12, pp. 304–313, 1988.

[54] N. Watanabe, T. Akasaka, Y. Yamaura, N. Kamiyama, M. Akiyama, Y. Koyama, Y. Neishi, and K. Yoshida, "Noninvasive assessment of great cardiac vein flow by Doppler echocardiography: A validation study," *J. Amer. Soc. Echocardiogr.*, vol. 15, no. 3, pp. 253–258, 2002.

[55] A. E. Weyman, *Principles and Practice of Echocardiography*, 2nd ed. Philadelphia, PA: Lea and Febiger, 1994.

[56] J. R. Womersley, "Method for the calculation of velocity, rate of flow and viscous drag in arteries when the pressure gradient is known," *J. Physiol.*, vol. 127, no. 3, pp. 553–563, 1955.

Authors' photographs and biographies not available at the time of publication.